NMR structure of the mouse prion protein domain PrP(121–231)

Roland Riek, Simone Hornemann, Gerhard Wider, Martin Billeter, Rudi Glockshuber & Kurt Wüthrich

Institut für Molekularbiologie und Biophysik, Eidgenössische Technische Hochschule-Hönggerberg, CH-8093 Zürich, Switzerland

THE 'protein only' hypothesis[1] states that a modified form of normal prion protein triggers infectious neurodegenerative diseases, such as bovine spongiform encephalopathy (BSE), or Creutzfeldt–Jakob disease (CJD) in humans[2–4]. Prion proteins are thought to exist in two different conformations[5]: the 'benign' PrP^C form, and the infectious 'scrapie form', PrP^{Sc}. Knowledge of the three-dimensional structure of PrP^C is essential for understanding the transition to PrP^{Sc}. The nuclear magnetic resonance (NMR) structure of the autonomously folding PrP domain comprising residues 121–231 (ref. 6) contains a two-stranded antiparallel β-sheet and three α-helices. This domain contains most of the point-mutation sites that have been linked, in human PrP, to the occurrence of familial prion diseases[7]. The NMR structure shows that these mutations occur within, or directly adjacent to, regular secondary structures. The presence of a β-sheet in PrP(121–231) is in contrast with model predictions of an all-helical structure of PrP^C (ref. 8), and may be important for the initiation of the transition from PrP^C to PrP^{Sc}.

The NMR structure of PrP(121–231) (Fig. 1*a* and Table 1) contains three α-helices and a two-stranded antiparallel β-sheet. The approximate lengths of the helices are from residues 144 to 154, 179 to 193, and 200 to 217, and the lengths of the β-strands are from residues 128 to 131, and 161 to 164. The first turn of the second helix and the last turn of the third helix are linked by the single disulphide bond in the protein. The twisted V-shaped arrangement of these two longest helices forms the scaffold onto which the short β-sheet and the first helix are anchored. At the present stage of refinement, all regular secondary-structure elements and the connecting loops are well defined (see Table 1 and Fig. 1*d*, *e*), with the sole exception of residues 167 to 176. The polypeptide fold is stabilized by hydrophobic interactions in a core that contains side chains of the second helix (residues 179, 180 and 184), the third helix (residues 203, 206, 209, 210, 213 and 214), the β-sheet (Val 161), the first, mostly hydrophilic, helix (Tyr 150), and three loop regions (residues 134, 137, 139, 141, 157, 158 and 198). With the exceptions of Ile 139, Ile 184 and Val 203, the residues of the hydrophobic core are invariant in the known mammalian prion protein sequences[9] (Fig. 3*a*). Hydrophobic surface patches in PrP(121–231) are located near the β-sheet and the loop preceding the first helix. The surface of PrP(121–231) is otherwise characterized by a markedly uneven distribution of positively and negatively charged residues (Fig. 1*b*, *c*).

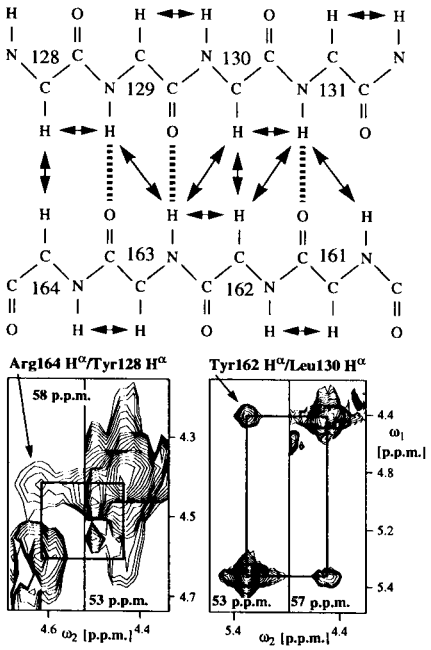

Mature mouse PrP^C is a glycosylated 208-residue protein (codons 23–231, with deletion of codon 55 (ref. 9)) that is attached to the cell surface by means of a glycosyl phosphatidyl inositol anchor at its carboxy-terminal Ser 231 (ref. 10). It seems to be necessary for normal synaptic function[11] (but see ref. 12), long-term survival of Purkinje neurons[13], and the regulation of circadian activity rhythms and sleep[14]. The segment of residues 109–218 was predicted to form a four-helix-bundle with helices at residues 109–122, 129–141, 178–191 and 202–218 (ref. 8), whereas prediction algorithms did not yield conclusive results for the segment 23–108, which contains the prion-characteristic octapeptide repeats. Attempts to express PrP(108–231) in the periplasm of *Escherichia coli* resulted in proteolytic cleavage after residues 112, 118 and 120, whereas PrP(121–231) is stable against degradation in *E. coli*, folds cooperatively and reversibly at pH 7 ($\Delta G_{Fold.} = -22\,kJ\,mol^{-1}$), and is soluble at 1 mM concentration in distilled water between pH 4.0 and pH 8.5 (ref. 6). This segment also contains six of nine point-mutation sites in mature PrP that have been associated with familial prion diseases[7] (Fig. 3*a*), as well as both glycosylation sites of PrP and its single disulphide bond[10]. We therefore chose to use PrP(121–231) for the present NMR structure determination. This choice was also supported by the demonstration that the segment 81–231 of mouse PrP is sufficient for propagation of the prion disease *in vivo*[15], indicating that the C-terminal part of PrP is of special functional importance.

In the context of the structure predictions for PrP^C (ref. 8), the β-sheet in the NMR structure of PrP(121–231) is an unexpected feature. Evidence for the identification of the β-sheet is shown in

TABLE 1 Parameters characterising the NMR structure determination of PrP(121–231)

Extent of assignments (backbone and side chain ^1H, $^{13}C^\alpha$, backbone ^{15}N)	93%
Number of distance constraints	1,368
Number of dihedral angle constraints	227
Distance constraint violations >0.1 Å (per conformer)	1.5 ± 1.3
Dihedral angle constraint violations > 2.5° (per conformer)	0.15 ± 0.36
Intra-protein AMBER energy (kcal mol^{-1})	−5,041 ± 97
R.m.s.d. to the mean for N, C^α and C′ of residues 125–166 and 177–219	1.4 Å
R.m.s.d. to the mean for all heavy atoms of residues 125–166 and 177–219	2.0 Å

The NMR structure of PrP(121–231) was calculated with the program DIANA[21]. Starting from 100 randomized structures, the 20 conformers with the lowest DIANA target function values were energy minimized in a water shell of 6 Å minimal thickness, using the program OPAL (P. Luginbühl, P. Güntert, M. Billeter and K. Wüthrich, submitted) with the AMBER force field[22].

◀FIG. 2 Identification of the antiparallel β-sheet in PrP(121–231). Top, β-sheet with arrows showing the NOEs from which this structure was identified before the structure calculation[16]. Broken lines indicate β-sheet hydrogen bonds for which slowed amide–proton exchange was observed. Bottom, spectral regions from a 3D ^{13}C-correlated [^{1}H, ^{1}H]-NOESY spectrum recorded in D_2O solution; squares connect the cross peaks and diagonal positions for the $d_{\alpha\alpha}(128, 164)$ and $d_{\alpha\alpha}(130, 162)$ connectivities.

Fig. 2, including the raw data on the two $d_{\alpha\alpha}$ interstrand nuclear Overhauser enhancement (NOE) connectivities, which are the most direct NMR identifiers of antiparallel β-structure[16]. Considering the proposed increase of the β-sheet content in PrP shown in transition from PrP^C to PrP^{Sc} (refs 5,17), it is tempting to speculate that the short β-sheet shown in Fig. 2 might be a 'nucleation site' for a conformational transition that could include the loops connecting the β-sheet to the first helix, which is predominantly hydrophilic and does not show amphipathic character. A systematic search of the Brookhaven data bank[18] with the program DALI[19] did not lead to the identification of other

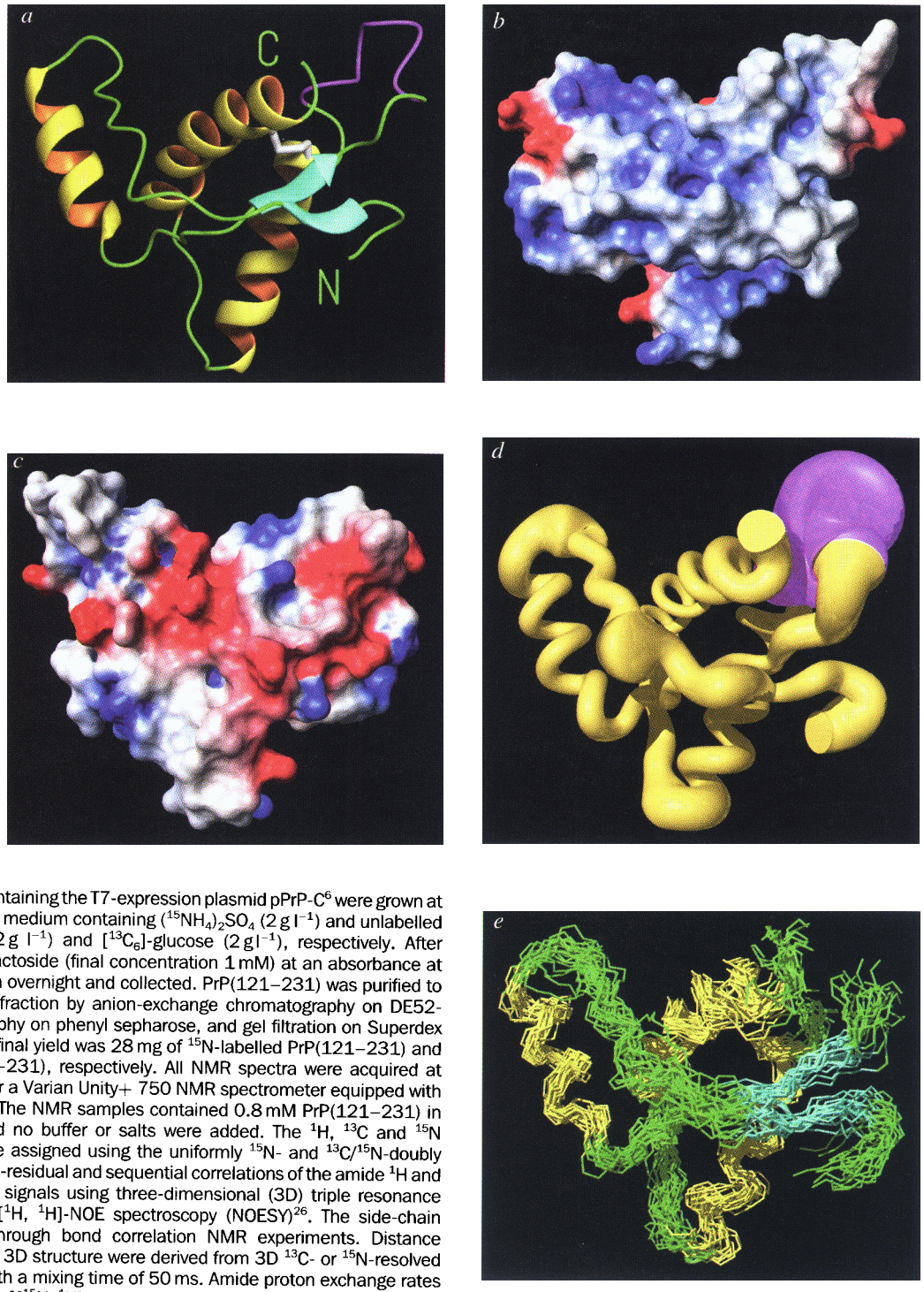

FIG. 1 Globular fold and surface properties of PrP(121–231). *a*, Ribbon diagram of the structure of the mouse prion protein domain PrP(121–231), indicating the positions of the three helices (yellow) and the antiparallel two-stranded β-sheet (cyan). The connecting loops are displayed in green if their structure is well defined, and in magenta otherwise. The disulphide bond between Cys 179 and Cys 214 is shown in white. The N-terminal segment of residues 121–124 and the C-terminal segment 220–231 are disordered and not displayed. *b*, *c*, Surface of the structure of PrP(121–231). Colours indicate the electrostatic potential[23], with blue for positive charges, red for negative charges. *b*, Same orientation as *a*. *c*, View after 180° rotation about a vertical axis. *d*, *e*, Representations of the precision of the structure determination. *d*, Display of the backbone of PrP(121–231) as a cylindrical rod of variable radius, which represents the global displacements among the 20 conformers used to represent the NMR structure (Table 1)[24]. Same orientation as *a*. Yellow represents residues 125–166 and 177–219, and the disordered loop of residues 167–176 is shown in magenta. *e*, Superposition of the 20 conformers; colours as in *a*.

METHODS. For the production of uniformly ^{15}N-labelled and ^{15}N/^{13}C-doubly labelled PrP(121–231), cells of *E. coli* BL21(DE3)[25] containing the T7-expression plasmid pPrP-C[6] were grown at room temperature in 10 l of minimal medium containing $(^{15}NH_4)_2SO_4$ (2 g l^{-1}) and unlabelled glucose (5 g l^{-1}) or $(^{15}NH_4)_2SO_4$ (2 g l^{-1}) and [$^{13}C_6$]-glucose (2 g l^{-1}), respectively. After induction with isopropyl-β-D-thiogalactoside (final concentration 1 mM) at an absorbance at 550 nm of 0.7, the cells were grown overnight and collected. PrP(121–231) was purified to homogeneity from the periplasmic fraction by anion-exchange chromatography on DE52-cellulose, hydrophobic chromatography on phenyl sepharose, and gel filtration on Superdex 200, as described elsewhere[6]. The final yield was 28 mg of ^{15}N-labelled PrP(121–231) and 16 mg of ^{13}C/^{15}N-labelled PrP(121–231), respectively. All NMR spectra were acquired at 20 °C either on a Bruker AMX 600 or a Varian Unity+ 750 NMR spectrometer equipped with triple-resonance *z*-gradient probes. The NMR samples contained 0.8 mM PrP(121–231) in 90% H_2O/10% D_2O at pH 4.5, and no buffer or salts were added. The ^{1}H, ^{13}C and ^{15}N resonances with the backbone were assigned using the uniformly ^{15}N- and ^{13}C/^{15}N-doubly labelled proteins by establishing intra-residual and sequential correlations of the amide ^{1}H and ^{15}N resonances with C^α, C^β and H^α signals using three-dimensional (3D) triple resonance experiments and 3D ^{15}N-resolved [^{1}H, ^{1}H]-NOE spectroscopy (NOESY)[26]. The side-chain signals were assigned from 3D through bond correlation NMR experiments. Distance constraints for the calculation of the 3D structure were derived from 3D ^{13}C- or ^{15}N-resolved [^{1}H, ^{1}H]-NOESY spectra recorded with a mixing time of 50 ms. Amide proton exchange rates were measured by recording a series of [^{15}N, ^{1}H]-correlation spectroscopy (COSY) experiments immediately after dissolving lyophilized PrP(121–231) in D_2O. The program MOLMOL[24] was used to generate the figure.

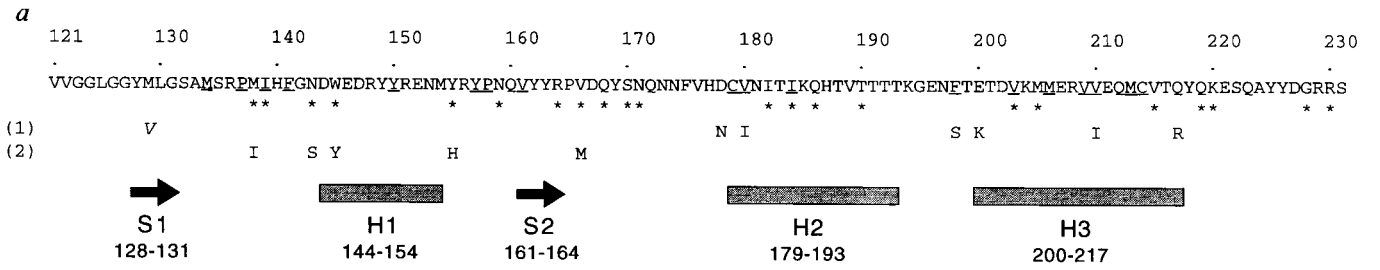

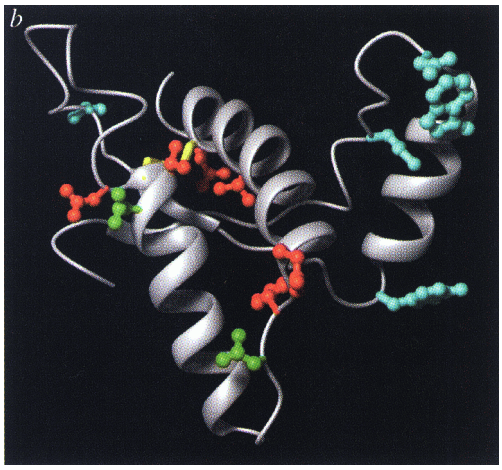

FIG. 3 Location in the 3D structure of PrP(121–231) of residues involved in sequence variations among mammalian prion proteins, and of residues that have been associated with the species barrier of prion disease transmission and with inherited prion diseases. *a*, Sequence and regular secondary structure of mouse PrP(121–231). Residues contributing to the hydrophobic core of the domain are underlined; variable residues among mammalian prion proteins[9] are marked with asterisks. Line (1), mutations in human PrP that have been associated with inherited prion diseases[7] (a stop codon at residue 145, which has been reported in addition to these point mutations[7], is not considered here, nor is the Met232Arg mutation[7], which is not contained in mature PrP^{C}). All of these residues are identical in wild-type human and mouse PrP. The polymorphism at codon 129 in human PrP, where homozygosity appears to increase susceptibility to sporadic CJD[7], is marked by italics. Line (2), residues in PrP(121–231) for which experimental evidence has been presented that they contribute to the species barrier of prion disease transmission between mice and humans[20]. *b*, Locations of selected residues in the three-dimensional structure of PrP(121–231). The backbone is shown in grey and the orientation of the molecule is as in Fig. 1c. The side chains of amino-acid residues with mutations that have been associated with inherited prion diseases[7] are highlighted in red (line (1) in *a*). The solvent-accessible glycosylation sites at Asn 181 and Asn 197 are shown in green, and the disulphide bond is shown in yellow. Five residues that may be involved in the species barrier (line (2) in *a*) are shown in blue. Figure generated using the program MOLMOL[24].

proteins with folds similar to PrP(121–231), and the relative orientation of the three helices in PrP(121–231) is clearly different from the proposed four-helix-bundle model[8].

Mapping onto the three-dimensional structure of PrP(121–231) of sequence variability in mammalian prion proteins[9], of residues important for the species barrier of prion disease transmission[20] and for predisposition to familial prion diseases[7], and of biochemical properties of the prion protein[6,10] (Fig. 3*a*, *b*) shows the following. (1) Invariant residues in mammalian prion protein sequences are not clustered within the regions of regular secondary structure, but form an important part of the hydrophobic core. (2) The two glycosylation sites at Asn 181 and Asn 197 and the solvent-exposed, single Trp 145 are located on the negatively charged surface of the protein. (3) All six residues of PrP(121–231) for which mutation is believed to be associated with inherited prion diseases or predisposition to prion diseases are located in regular secondary structure elements or immediately adjacent to them, but none of these residues is located in the relatively isolated first helix. Three of these residues are part of the hydrophobic core, and three are located on the surface. They may therefore either destabilize the three-dimensional protein structure, or influence its ligand-binding properties. (4) As is generally observed for functionally related proteins from different species, residues in PrP(121–231) that are variant in mammalian prion protein sequences[9] are solvent accessible. (5) The disulphide bond 179–214 is highly shielded from solvent contact in the core of the protein.

It has been proposed that the species barrier of prion disease transmission between mice and humans is caused by an altered PrP^{Sc} binding site in PrP^{C}, which involves residues from the segment 96–167 (ref. 20). There are eight sequence differences between mouse and human PrP within this segment, of which five are contained in PrP(121–231). Four of these differences are located within or adjacent to the first helix, which might thus be part of a single binding site for PrP^{Sc} (Fig. 3*a*, *b*). The dipolar character of PrP(121–231) (Fig. 1*b*, *c*) might stabilize an orientation of PrP^{C} with its positively charged surface, which also includes hydrophobic surface patches, towards the cell membrane. Both glycosylation sites, as well as the aforementioned species barrier-related potential binding site for PrP^{Sc}, would then be located on the opposite, negatively charged surface. Further to these initial observations on possible structure–function correlations, we believe that the NMR structure of PrP(121–231) will provide a basis for more rational design of future *in vitro* and *in vivo* experiments on prion proteins and prion diseases. □

Received 13 May; accepted 5 June 1996.

1. Griffith, J. S. *Nature* **215,** 1043–1044 (1967).
2. Prusiner, S. B. *Science* **252,** 1515–1522 (1991).
3. Weissmann, C. *Trends Cell Biol.* **4,** 10–14 (1994).
4. Weissmann, C. *Nature* **375,** 628–629 (1995).
5. Pan, K.-M. *et al. Proc. natn. Acad. Sci. U.S.A.* **90,** 10962–10966 (1993).
6. Hornemann, S. & Glockshuber, R. *J. molec. Biol.* (in the press).
7. Prusiner, S. B. *Arch. Neurol.* **50,** 1129–1153 (1993).
8. Huang, Z. *et al. Proc. natn. Acad. Sci. U.S.A.* **91,** 7139–7143 (1994).
9. Schätzl, H. M., Da Costa, M., Taylor, L., Cohen, F. E. & Prusiner, S. B. *J. molec. Biol.* **245,** 362–374 (1995).
10. Stahl, N. & Prusiner, S. B. *FASEB J.* **5,** 2799–2807 (1991).
11. Collinge, J. *et al. Nature* **370,** 295–297 (1994).
12. Lledo, P.-M. *et al. Proc. natn. Acad. Sci. U.S.A.* **93,** 2403–2407 (1996).
13. Sakaguchi, S. *et al. Nature* **380,** 528–531 (1996).
14. Tobler, I. *et al. Nature* **380,** 639–642 (1996).
15. Fischer, M. *et al. EMBO J.* **15,** 1255–1264 (1996).
16. Wüthrich, K. *NMR of Proteins and Nucleic Acids* (Wiley, New York, 1986).
17. Huang, Z., Prusiner, S. B. & Cohen, F. E. *Fold. Design* **1,** 13–19 (1996).
18. Bernstein *et al. J. molec. Biol.* **112,** 535–542 (1977).
19. Holm, L. & Sander, C. *Proteins* **19,** 165–173 (1994).
20. Telling, G. C. *et al. Cell* **83,** 79–90 (1995).
21. Güntert, P., Braun, W. & Wüthrich, K. *J. molec. Biol.* **217,** 517–530 (1991).
22. Cornell *et al. J. Am. chem. Soc.* **117,** 5179–5197 (1995).
23. Honig, B. & Nicholls, A. *Science* **268,** 1144–1149 (1994).
24. Koradi, R., Billeter, M. & Wüthrich, K. *J. molec. Graph.* **14,** 51–55 (1996).
25. Studier, F. W. & Moffat, B. A. *J. molec. Biol.* **189,** 113–130 (1986).
26. Cavanagh, J., Fairbrother, W. J., Palmer, A. G. & Skelton, N. J. *Protein NMR Spectroscopy, Principles and Practice* (Academic, San Diego, 1996).

ACKNOWLEDGEMENTS. We thank M. Fischer, A. Raeber, C. Mumenthaler, and C. Weissmann for discussions, and the Centro Svizzero di Calculo Scientifico for use of the NEC SX-3 and Cray J-90 computers. This work was supported by the Schweizerischer Nationalfonds and the ETH Zürich. S.H. was supported by the Boehringer-Ingelheim-Fonds.

CORRESPONDENCE and requests for materials should be addressed to R.G. (e-mail: rudi@mol.biol.ethz.ch).